Journal of Multidisciplinary Engineering Science and Technology (JMEST)
ISSN: 3159-0040
Vol. 2 Issue 2, February - 2015

Numerical Solution of the Axisymmetric Stagnation Flow of Micropolar Fluid Towards a Shrinking Sheet by SOR Iterative Procedure

Dr. Mohammad Shafique

Ex-AP, Department of Mathematics, Gomal University, D I Khan, Pakistan
Current: Private Teaching in Mathematics, Toronto ON, Canada
Emails: mshafique6161@yahoo.com and mshafique6161@hotmail.com

ABSTRACT—The problem of the axisymmeteric stagnation flows of micropolar fluids towards a shrinking sheet has been solved numerically. The similarity transformations have been used to reduce the highly nonlinear partial differential equations of motion to ordinary differential equations. The resulting equations are then solved by using by SOR iterative procedure. The results have been calculated on three different grid sizes to check the accuracy of the results. The numerical results have been obtained for various values of the parameter α for the range -1.1 to 10. For positive values, the problem relates to the stagnation flow towards a stretching sheet. For negative values, the problem relates to the flow towards a shrinking sheet. The results computed for micropolar case are found in good agreement with those obtained with the Newtonian results.

Keywords—Micropolar Fluids, Shrinking Sheet and SOR Iterative Procedure

1. INTRODUCTION

In the past, the researchers have been engaged in the study of stretching phenomenon but during the last few years, the investigators are involved to solve the flow problems related to shrinking surface due to its importance in extrusion processes.

The flow problems of stretching surfaces have relevance to several technological processes. Chiam [1] investigated steady two dimensional stagnation point flow of an incompressible fluid towards a stretching surface. Ishak et al [2] analyzed the mixed convection boundary layers in the stagnation point flow toward a stretching vertical sheet. Flow of an electrically conducting non- Newtonian fluid past a stretching surface was studied by Able et al [3] when a uniform magnetic field acts transverse to the surface. Ishak et al [4] investigated the steady two-dimensional MHD stagnation flow towards a stretching sheet with variable surface temperature and obtained numerical results using the Keller-box method. Wang [5] considered the axisymmeteric stagnation flows towards a shrinking sheet.

The MHD boundary layer flow of fluid over a shrinking sheet has been studied by Hayat et al [6] and Fang [7]. Nadeem et al [8] and Ara et al [9] have been investigated MHD boundary layer flow of fluid over an exponentially permeable shrinking sheet. The steady boundary layer flow and steady two-dimensional flow of a nanofluid past a nonlinearly permeable stretching/ shrinking sheet is numerically studied by Zaimi et al [10, 11]. Sajid and Hayat [12] applied homotopy analysis method for MHD viscous flow due to a shrinking sheet. The problem of [12] is studied by Noor et al. [13] by using simple non-perturbative method. Shafique et al [14] have been studied the problem numerical solutions of MHD viscous flow of micropolar fluids due to a shrinking sheet numerically by using SOR iterative procedure.

Wang [5] has found the results for the range $-1 \le \alpha \le 5.0$ and concluded that no solution exists for $\alpha < -1$. We intend to give an extention to this problem for the range $-1.1 \le \alpha \le 10$. This particular range of parameter α has been taken in view of convergence of our numerical scheme. We concluded that the solution exists in the extended range of parameter α. This shows that our numerical scheme is better than that of previous one

In this research, the axisymmetric stagnation point flow of micropolar fluid towards a shrinking sheet is considered. The similarity transformations have been used to reduce the highly nonlinear partial differential equations of motion to ordinary differential equations. The resulting equations are then solved by using by SOR iterative procedure with Simpson's (1/3) rule [15]. The numerical results have been obtained for different values of the flow parameters namely α and Prandtl number Pr. When $\alpha > 0$ the problem corresponds to the case of stretching sheet and for $\alpha < 0$, the problem corresponds to shrinking sheet. The results computed for micropolar case are found in good agreement with those obtained with the Newtonian results.

2. MATHEMATICAL ANALYSIS

The micropolar fluids flow is assumed to be steady, laminar and incompressible. The body force, the body couples and the viscous dissipation are neglected. The Cartesians coordinate axes are preferred to cylindrical coordinate axes because of the possible non- alignment. The flow field is three dimensional. The stretching axis and the stagnation flow are not aligned in general. The distance between the axis of the stagnation flow and the center of the shrinking surface is *c*.

Under these assumptions, the equations of motion for micropolar fluids flow become:

$$\frac{\partial u}{\partial x}+\frac{\partial v}{\partial y}+\frac{\partial w}{\partial z}=0, \tag{1}$$

$$(\mu+\kappa)\left(\frac{\partial^2 u}{\partial x^2}+\frac{\partial^2 u}{\partial y^2}+\frac{\partial^2 u}{\partial z^2}\right)+\kappa\left(\frac{\partial \omega_3}{\partial y}-\frac{\partial \omega_2}{\partial z}\right)$$
$$-\frac{\partial \pi}{\partial x}=\rho\left(u\frac{\partial u}{\partial x}+v\frac{\partial u}{\partial y}+w\frac{\partial u}{\partial z}\right), \tag{2}$$

$$(\mu+\kappa)\left(\frac{\partial^2 v}{\partial x^2}+\frac{\partial^2 v}{\partial y^2}+\frac{\partial^2 v}{\partial z^2}\right)+\kappa\left(\frac{\partial \omega_1}{\partial z}-\frac{\partial \omega_3}{\partial x}\right)$$
$$-\frac{\partial \pi}{\partial y}=\rho\left(u\frac{\partial v}{\partial x}+v\frac{\partial v}{\partial y}+w\frac{\partial v}{\partial z}\right), \tag{3}$$

$$(\mu+\kappa)\left(\frac{\partial^2 w}{\partial x^2}+\frac{\partial^2 w}{\partial y^2}+\frac{\partial^2 w}{\partial z^2}\right)+\kappa\left(\frac{\partial \omega_2}{\partial x}-\frac{\partial \omega_1}{\partial y}\right)$$
$$-\frac{\partial \pi}{\partial z}=\rho\left(u\frac{\partial w}{\partial x}+v\frac{\partial w}{\partial y}+w\frac{\partial w}{\partial z}\right), \tag{4}$$

$$(\alpha+\beta+\gamma)\left(\frac{\partial}{\partial x}\left(\frac{\partial \omega_1}{\partial x}+\frac{\partial \omega_2}{\partial y}+\frac{\partial \omega_3}{\partial z}\right)\right)$$
$$-\gamma\left(\frac{\partial}{\partial x}\left(\frac{\partial \omega_1}{\partial x}+\frac{\partial \omega_2}{\partial y}+\frac{\partial \omega_3}{\partial z}\right)-\left(\frac{\partial^2 \omega_1}{\partial x^2}+\frac{\partial^2 \omega_1}{\partial y^2}+\frac{\partial^2 \omega_1}{\partial z^2}\right)\right) \tag{5}$$
$$+\kappa\left(\frac{\partial w}{\partial y}-\frac{\partial v}{\partial z}\right)-2\kappa\omega_1=\rho j\left(u\frac{\partial \omega_1}{\partial x}+v\frac{\partial \omega_1}{\partial y}+w\frac{\partial \omega_1}{\partial z}\right),$$

$$(\alpha+\beta+\gamma)\left(\frac{\partial}{\partial y}\left(\frac{\partial \omega_1}{\partial x}+\frac{\partial \omega_2}{\partial y}+\frac{\partial \omega_3}{\partial z}\right)\right)$$
$$-\gamma\left(\frac{\partial}{\partial y}\left(\frac{\partial \omega_1}{\partial x}+\frac{\partial \omega_2}{\partial y}+\frac{\partial \omega_3}{\partial z}\right)-\left(\frac{\partial^2 \omega_2}{\partial x^2}+\frac{\partial^2 \omega_2}{\partial y^2}+\frac{\partial^2 \omega_2}{\partial z^2}\right)\right) \tag{6}$$
$$+\kappa\left(\frac{\partial u}{\partial z}-\frac{\partial w}{\partial x}\right)-2\kappa\omega_2=\rho j\left(u\frac{\partial \omega_2}{\partial x}+v\frac{\partial \omega_2}{\partial y}+w\frac{\partial \omega_2}{\partial z}\right),$$

$$(\alpha+\beta+\gamma)\left(\frac{\partial}{\partial z}\left(\frac{\partial \omega_1}{\partial x}+\frac{\partial \omega_2}{\partial y}+\frac{\partial \omega_3}{\partial z}\right)\right)$$
$$-\gamma\left(\frac{\partial}{\partial z}\left(\frac{\partial \omega_1}{\partial x}+\frac{\partial \omega_2}{\partial y}+\frac{\partial \omega_3}{\partial z}\right)-\left(\frac{\partial^2 \omega_3}{\partial x^2}+\frac{\partial^2 \omega_3}{\partial y^2}+\frac{\partial^2 \omega_3}{\partial z^2}\right)\right) \tag{7}$$
$$+\kappa\left(\frac{\partial v}{\partial x}-\frac{\partial u}{\partial y}\right)-2\kappa\omega_3=\rho j\left(u\frac{\partial \omega_3}{\partial x}+v\frac{\partial \omega_3}{\partial y}+w\frac{\partial \omega_3}{\partial z}\right),$$

$$\rho C_p\left(u\frac{\partial T}{\partial x}+v\frac{\partial T}{\partial y}+w\frac{\partial T}{\partial z}\right)=K\left(\frac{\partial^2 T}{\partial x^2}+\frac{\partial^2 T}{\partial y^2}+\frac{\partial^2 T}{\partial z^2}\right). \tag{8}$$

We look for a solution in which the velocity and microrotation vectors may be written in the following form:

$\underline{V}=V(u(x,y,z),v(x,y,z),w(x,y,z))$ and $\underline{\omega}=\omega(\omega_1(x,y,z),\omega_2(x,y,z),0)$.

We used the following similarity transformations to obtain the governing partial differential equations (1) to (8) in ordinary differential form.

$$u=axf'(\eta)+bcg(\eta),\quad v=ayf'(\eta),\quad w=-2\sqrt{av}\,f(\eta),$$
$$\omega_1=-ay\sqrt{a/\nu}L(\eta),\quad \omega_2=\sqrt{a/\nu}(axL(\eta)+bcM(\eta)), \tag{9}$$
$$\omega_3=0 \text{ and } \theta(\eta)=\frac{T-T_\infty}{T_0-T_w},$$

where $\eta=\sqrt{\frac{a}{\nu}}z$ is a non dimensional variable, *c* is the distance between the axis of stagnation flow and the center of shrinking surface and *b* is shrinking rate and *b*<0 indicates the shrinking surface.

From equation (4), the pressure π is obtained as:

$$\pi=\pi_0-\rho a^2\frac{x^2}{2}-\rho a^2\frac{y^2}{2}-\rho\frac{w^2}{2}+\rho\nu\frac{\partial w}{\partial z}.$$

The equation of continuity (1) is satisfied and the equations (2) to (8) lead to:

$$f'''-C_1L'+1=f'^2-2ff'', \tag{10}$$
$$g''-C_1M'=gf'-2g'f, \tag{11}$$
$$L''+C_2(f''-2L)=C_3(fL-2fL'), \tag{12}$$
$$M''+C_2(g'-2M)=C_3(gL-2fM') \tag{13}$$
$$\theta''+\Pr f\theta'=0. \tag{14}$$

Here C_1, C_2, C_3 are dimensionless constants in the form

$$C_1=\frac{\kappa}{\mu+\kappa}, C_2=\frac{\kappa\upsilon}{\gamma a} \text{ and } C_3=\frac{\rho j\upsilon}{\gamma}.$$

The dimensions of the parameters involved are as follows

$$[\mu,\kappa]=MT^{-1}L^{-1},[\gamma]=MLT^{-1},[j]=L^2,$$
$$[\rho]=ML^{-3},[a]=T^{-1}\text{and}[\nu]=L^2T^{-1}.$$

The boundary conditions are:

$$f=0, f'=\alpha, g=1, L=0, M=0, \theta=1, \quad \text{at } \eta=0,$$
$$f'\to 1, g\to 0, L\to 0, M\to 0, \theta\to 0, \quad \text{as } \eta\to\infty. \tag{15}$$

Where $\alpha=\frac{b}{a}$, $\Pr=\frac{\rho\nu C_p}{K}$ and $\nu=\frac{\mu}{\rho}$ is the coefficient of kinematic viscosity. The primes denote the differentiation with respect to η.

3. FINITE DIFFERENCE EQUATIONS

In order to solve the equations (10) to (14) numerically, we set

$$P=f'. \tag{16}$$

Then equations (10) to (14) become:

$$P''-C_1L'+1=P^2-2P'f\ , \tag{17}$$

$$g''-C_1M'=gP-2g'f\ , \tag{18}$$

$$L''+C_2(P'-2L)=C_3(PL-2fL')\ , \tag{19}$$

$$M''+C_2(g'-2M)=C_3(gL-2fM')\ , \tag{20}$$

$$\theta''+\Pr f\theta'=0. \tag{21}$$

The boundary conditions (15) become:

$$f=0,P=\alpha,g=1,L=0,M=0,\theta=1,\text{at}\ \eta=0,$$
$$P\to 1,g\to 0,L\to 0,M\to 0,\theta\to 0,\text{as}\ \eta\to\infty. \tag{22}$$

We now approximate the derivatives in equations (17) to (21) by central-difference approximations at a typical grid point $\eta_n=nh$ of the interval [0,∞) and we obtain:

$$(2+2hf_n)P_{n+1}+(2-2hf_n)P_{n-1}+2h^2$$
$$-C_1(L_{n+1}-L_{n-1})-(4+2h^2P_n)P_n=0\ , \tag{23}$$

$$(2+2hf_n)g_{n+1}+(2-2hf_n)g_{n-1}$$
$$-C_1h(M_{n+1}-M_{n-1})-(4+2h^2p_n)g_n=0 \tag{24}$$

$$(2+2C_3hf_n)L_{n+1}+(2-2C_3hf_n)L_{n-1}$$
$$+C_2h(P_{n+1}-P_{n-1})=(4+C_2 4h^2+C_3 2h^2P_n)L_n, \tag{25}$$

$$(2+2C_3hf_n)M_{n+1}+(2-2C_3hf_n)M_{n-1}$$
$$+C_2h(g_{n+1}-g_{n-1})=2h^2C_3g_nL_n+(4+C_2 4h^2)M_n, \tag{26}$$

$$2(\theta_{n+1}+\theta_{n-1})+\Pr f_nh(\theta_{n+1}-\theta_{n-1})=4\theta_n \tag{27}$$

where *h* denotes a grid size and $f_n=f(\eta_n)$, $g_n=g(\eta_n)$, $P_n=P(\eta_n)$, $L_n=L(\eta_n)$, $M_n=M(\eta_n)$ and $\theta_n=\theta(\eta_n)$. For computational purpose, we shall replace the interval [0, ∞) by [0, β), where β is sufficiently large.

4. COMPUTATIONAL PROCEDURE

We now solve numerically the first order ordinary differential equation (16) and the system of finite difference equations (23) to (27) at each interior grid point of the interval. The equation (16) is integrated by the Simpson's (1/3) rule, whereas the set of equations (23) to (27) are solved by using SOR iterative procedure subject to the appropriate conditions.

The order of the sequence of iterations is as follows:

1. The equations (23) and (27) are solved to calculate the values of *P, g, L, M* and θ subject to the boundary conditions:
   $P=\alpha,g=1,\theta=1,L=0,M=0,\text{when}\ \eta=0,$
   $P=1,g=0,\theta=0,L=0,M=0,\text{when}\ \eta\to\infty.$
2. The computed solutions of *P* are then employed into the equation (16) for the calculation of *f* with the condition:
   $f=0,\quad \text{when}\quad \eta=0.$
3. In order to accelerate the speed of convergence of the SOR method, the optimum value of the relaxation parameter ω_{opt} is estimated between 1 and 2. The optimum value of the relaxation parameter for the problem under consideration is 1.5.
4. The above procedure is repeated until convergence is obtained according to the criterion $\max\left|U^{n+1}-U^n\right|<10^{-6}$ where *n* denotes the number of iterations and *U* stands for each of the functional value.

For higher order accuracy, the above steps 1 to 4 are repeated for step sizes $\frac{h}{2}$ and $\frac{h}{4}$.

5. DISCUSSION ON NUMERICAL RESULTS

The calculations were made for different values of parameter α in the range $-1.10\le\alpha\le 10$ and Pr=0.7. The results have been obtained for the following grid sizes *h*=0.01, 0.005, 0.0025. The computations for different grids sizes facilitated the comparison and accuracy of the numerical results. Excellent comparison and higher order accuracy have been achieved by the numerical methods used herein.

The values of the parameters C_1, C_2 and C_3 have been chosen arbitrarily in the form of three different sets given in the table below:

Case	C_1	C_2	C_3
I	0.02	0.5	1.5
II	0.05	1.2	0.7
III	0.1	0.5	1.5

If the above constants are zero, the micropolar fluids flow becomes the Newtonian fluids flow. The three different cases for the values of the constants have been considered for this micropolar fluids flow problem during the computational work. When C_1 is small and C_2, C_3 are large, the micropolar fluids flow resembles with Newtonian fluids flow as in Case-I. The cases II and III are far from the results of Newtonian fluids due to fast miro rotation of the molecules because of large values of material constants.

The results for the flow functions f, f', non-alignment function g, heat function θ, micropolar functions *L* and *M* have been presented in the Table 1 to Table 5 in the case-I of the material constants for each of grid sizes. The results for $f''(0)$ and $g'(0)$ have been obtained for the above range of α. The comparison of present results for micropolar fluids, Newtonian fluids and the previous results by Wang [5] is given in Table 6 and Table 7, where possible.

Graphical behavior of the velocity function $f(\eta)$ is shown in Figure 1 and Figure 2 for non negative and negative values of α respectively. The curve for

$\alpha = 0$ indicates the flow behavior similar to the axisymmetric stagnation flow of micropolar fluids and for $\alpha = 1$, it corresponds to inviscid flow without boundary layer. For higher positive values of α, the curves for the function $f(\eta)$ raise higher. For negative values of α, the curves of $f(\eta)$ are initially negative. The situation depicts the regions of reverse flow in cellular form.

Figure 3 exhibits the function $g(\eta)$ for different values of α. The initial values of $f''(0), g'(0)$ have been plotted in Figure 4 and Figure 5 respectively.

The function $-\theta'(0)$ showing heat loss at the surface has been demonstrated in Figure 6. It is noticed that $-\theta'(0)$ decreases accordingly, as the thickness of the boundary is increased in case the shrinking is increased.

.

Table 1: The functions f, f', g, θ, L, M in the case-I for α =0.0

h	η	*f*	f'	*g*	θ	*L*	*M*
0.010	0.000	0.000000	0.000000	1.000000	1.000000	0.000000	0.000000
	1.000	0.492507	0.830142	0.233123	0.374857	0.040649	-0.061676
	2.000	1.433385	0.992104	0.014015	0.055065	0.002529	-0.004804
	3.000	2.431680	1.000136	0.000156	0.002446	0.000007	-0.000037
	4.000	3.431834	1.000119	0.000000	0.000030	-0.000005	0.000000
	5.000	4.431892	1.000000	0.000000	0.000000	0.000000	0.000000
0.005	0.000	0.000000	0.000000	1.000000	1.000000	0.000000	0.000000
	1.000	0.492638	0.830280	0.175907	0.243228	0.036059	-0.045450
	2.000	1.433515	0.991928	0.007042	0.018848	0.002300	-0.002452
	3.000	2.431448	0.999718	0.000053	0.000417	0.000017	-0.000013
	4.000	3.431257	0.999866	0.000000	0.000003	0.000004	0.000000
	5.000	4.431176	1.000000	0.000000	0.000000	0.000000	0.000000
0.0025	0.000	0.000000	0.000000	1.000000	1.000000	0.000000	0.000000
	1.000	0.492723	0.830422	0.007643	0.019704	0.002628	-0.002675
	2.000	1.433681	0.991949	0.000000	0.000004	0.000022	0.000000
	3.000	2.431624	0.999722	0.000000	0.000000	0.000000	0.000000
	4.000	3.431439	0.999870	0.000000	0.000000	0.000000	0.000000
	5.000	4.431363	1.000000	0.000000	0.000000	0.000000	0.000000

Table 2: The functions f, f', g, θ, L, M in the case-I for α =5.0

h	η	*f*	f'	*g*	θ	*L*	*M*
0.010	0.000	0.000000	5.000000	1.000000	1.000000	0.000000	0.000000
	1.000	2.117132	1.069409	0.020931	0.073831	-0.013242	-0.004167
	2.000	3.130185	1.000280	0.000066	0.001339	-0.000035	-0.000011
	3.000	4.130360	1.000159	0.000000	0.000006	-0.000001	0.000000
	4.000	5.130484	1.000082	0.000000	0.000000	-0.000002	0.000000
	5.000	6.130524	1.000000	0.000000	0.000000	0.000000	0.000000
0.005	0.000	0.000000	5.000000	1.000000	1.000000	0.000000	0.000000
	1.000	2.117075	1.069400	0.015873	0.042932	-0.012682	-0.003119
	2.000	3.130091	1.000137	0.000029	0.000303	-0.000029	-0.000005
	3.000	4.130067	0.999924	0.000000	0.000000	0.000000	0.000000
	4.000	5.129960	0.999909	0.000000	0.000000	0.000002	0.000000
	5.000	6.129907	1.000000	0.000000	0.000000	0.000000	0.000000
0.0025	0.000	0.000000	5.000000	1.000000	1.000000	0.000000	0.000000
	1.000	2.116703	1.069312	0.000330	0.001336	-0.002242	-0.000069
	2.000	3.129747	1.000235	0.000000	0.000000	-0.000007	0.000000
	3.000	4.129804	0.999977	0.000000	0.000000	-0.000001	0.000000
	4.000	5.129733	0.999965	0.000000	0.000000	0.000000	0.000000
	5.000	6.129741	1.000000	0.000000	0.000000	0.000000	0.000000

Table 3: The functions f, f', g, θ, L, M in the case-I for α =10.0

h	η	*f*	f'	*g*	θ	*L*	*M*
0.010	0.000	0.000000	10.000000	1.000000	1.000000	0.000000	0.000000
	1.000	2.933429	1.040052	0.005171	0.028018	-0.006661	-0.000835
	2.000	3.939450	1.000167	0.000004	0.000174	-0.000525	0.000000

	3.000	4.939616	1.000152	0.000000	0.000000	-0.000024	0.000000
	4.000	5.939728	1.000072	0.000000	0.000000	-0.000003	0.000000
	5.000	6.939764	1.000000	0.000000	0.000000	0.000000	0.000000
0.005	0.000	0.000000	10.000000	1.000000	1.000000	0.000000	0.000000
	1.000	2.933523	1.040061	0.004267	0.017409	-0.006215	-0.000687
	2.000	3.939478	0.999995	0.000002	0.000043	-0.000002	0.000000
	3.000	4.939441	0.999930	0.000000	0.000000	0.000000	0.000000
	4.000	5.939353	0.999920	0.000000	0.000000	0.000002	0.000000
	5.000	6.939302	1.000000	0.000000	0.000000	0.000000	0.000000
0.0025	0.000	0.000000	10.000000	1.000000	1.000000	0.000000	0.000000
	1.000	2.933047	1.040004	0.000169	0.000771	-0.002483	-0.000028
	2.000	3.939111	1.000164	0.000000	0.000000	-0.000002	0.000000
	3.000	4.939214	1.000043	0.000000	0.000000	-0.000002	0.000000
	4.000	5.939237	1.000040	0.000000	0.000000	-0.000001	0.000000
	5.000	6.939303	1.000000	0.000000	0.000000	0.000000	0.000000

Table 4: The functions f, f', g, θ, L, M in the case-I for α =-0.50

h	η	*f*	f'	*g*	θ	*L*	*M*
0.010	0.000	0.000000	-0.500000	1.000000	1.000000	0.000000	0.000000
	1.000	0.116527	0.600617	0.385406	0.514381	0.091385	-0.098042
	2.000	0.947045	0.962200	0.047983	0.126697	0.013725	-0.019473
	3.000	1.936392	0.999400	0.001266	0.010368	0.000230	-0.000396
	4.000	2.936427	1.000136	0.000006	0.000240	-0.000005	-0.000001
	5.000	3.936492	1.000000	0.000000	0.000000	0.000000	0.000000
0.005	0.000	0.000000	-0.500000	1.000000	1.000000	0.000000	0.000000
	1.000	0.116897	0.601186	0.168259	0.228079	0.052984	-0.049300
	2.000	0.947792	0.962358	0.005774	0.013086	0.006735	-0.002633
	3.000	1.937121	0.999201	0.000038	0.000188	0.000161	-0.000014
	4.000	2.936952	0.999949	0.000000	0.000001	0.000000	0.000000
	5.000	3.936896	1.000000	0.000000	0.000000	0.000000	0.000000
0.0025	0.000	0.000000	-0.500000	1.000000	1.000000	0.000000	0.000000
	1.000	0.116970	0.601385	0.006368	0.013931	0.007241	-0.002889
	2.000	0.948028	0.962441	0.000000	0.000001	0.000058	0.000000
	3.000	1.937381	0.999202	0.000000	0.000000	0.000002	0.000000
	4.000	2.937217	0.999953	0.000000	0.000000	0.000000	0.000000
	5.000	3.937165	1.000000	0.000000	0.000000	0.000000	0.000000

Table 5: The functions f, f', g, θ, L, M in the case-I for α =-1.10

h	η	*f*	f'	*g*	θ	*L*	*M*
0.010	0.000	0.000000	-1.100000	1.000000	1.000000	0.000000	0.000000
	1.000	-1.232394	-1.354822	2.200687	0.997685	-0.034158	0.164442
	2.000	-2.704252	-1.590822	3.108001	0.996425	-0.053547	0.223086
	3.000	-4.423356	-1.854164	3.944039	0.995919	-0.075575	0.272010
	4.000	-6.429314	-2.167514	4.795180	0.995852	-0.103776	0.328327
	5.000	-8.567269	1.000000	0.000000	0.000000	0.000000	0.000000
0.005	0.000	0.000000	-1.100000	1.000000	1.000000	0.000000	0.000000
	1.000	-1.405577	-1.696998	2.790320	0.999272	-0.130405	0.330694
	2.000	-3.380602	-2.250956	4.248663	0.998791	-0.205524	0.493899
	3.000	-5.908284	-2.806603	5.593187	0.998539	-0.270990	0.628165
	4.000	-9.000560	-3.382269	6.898392	0.998384	-0.336247	0.757621
	5.000	-12.47815	1.000000	0.000000	0.000000	0.000000	0.000000
0.0025	0.000	0.000000	-1.100000	1.000000	1.000000	0.000000	0.000000
	1.000	-1.450018	-1.783575	3.855350	0.999255	-0.191393	0.593209
	2.000	-3.549065	-2.409941	6.272112	0.995629	-0.308495	0.927208
	3.000	-6.265245	-3.021636	8.477535	0.984190	-0.405607	1.211051
	4.000	-9.592555	-3.633810	10.561618	0.966048	-0.494534	1.475982
	5.000	-13.33376	1.000000	0.000000	0.000000	0.000000	0.000000

Table 6: The comparison of Micropolar fluids and Newtonian fluids for $f''(0)$

α	Micropolar fluids			Newtonian fluids	
	I	II	III	Present Results	Results of Wang[5]
0	1.3116185	1.3085542	1.3092093	1.3122251	1.311938
0.1	1.2287378	1.2267599	1.2266874	1.2292832	1.22911
0.2	1.1335313	1.1314034	1.1320650	1.1339485	1.13374
0.5	0.7801294	0.7776499	0.7788658	0.7805824	0.78032
1.0	-0.0004053	-0.0000238	-0.00045299	-0.95367431	0
2.0	-2.127266	-2.127218	-2.127457	-2.126980	-2.13107
5.0	-11.778642	-11.768914	-11.771394	-11.776734	-11.8022
8.0	-25.024604	-25.013160	-25.018310	-25.026512	-----
10.0	-35.44922	-35.44006	-35.44464	-35.45265	-----
-0.05	1.3482958	1.3455361	1.3454899	1.3486698	-----
-0.15	1.4100134	1.4067113	1.4067769	1.4107167	-----
-0.25	1.4542669	1.4522910	1.4531314	1.4570951	1.45664
-0.50	1.4891862	1.4787912	1.4841437	1.4901995	1.49001
-0.75	1.3496756	-1.3152122	1.3431549	1.3530015	1.35284
-0.95	0.9406328	0.9273529	0.9221792	0.9458780	0.94690
-0.9945	0.6399632	0.5864143	0.5809069	0.6551266	0.5
-1.0	0.5525589	0.4981041	0.4347324	0.6350279	0
-1.10	-0.7450104	1.3161136	-0.8996487	-1.0703086	-----

Table 7: The comparison of Micropolar fluids and Newtonian fluids for $g'(0)$

α	Micropolar fluids			Newtonian fluids	
	I	II	III	Present Results	Results of Wang[5]
0	-0.9378612	-0.9342015	-0.9339511	-0.9386957	-0.93873
0.1	-1.0027229	-0.9991586	-0.9989500	-1.0035276	-1.0040
0.2	-1.0641992	-1.0607361	-1.0605990	-1.0649502	-1.0659
0.5	-1.2323617	-1.2290418	-1.2290954	-1.2329936	-1.2355
1.0	-1.4735519	-1.4705657	-1.4707684	-1.4740705	-1.4793
2.0	-1.8695175	-1.8559307	-1.8672943	-1.8699347	-1.8800
5.0	-2.736425	-2.734423	-2.734852	-2.736712	-2.7617
8.0	-3.386772	-3.385127	-3.385532	-3.387072	-----
10.0	-3.756851	-3.755355	-3.755754	-3.757072	-----
-0.05	-0.9040237	-0.9002686	-0.8999586	-0.9048998	-----
-0.15	-0.8329094	-0.8290708	-0.8286774	-0.8338392	-----
-0.25	-0.7566452	-0.7525385	-0.7519960	-0.7576227	-0.75639
-0.50	-0.5335868	-0.5290091	-0.5278945	-0.5349279	-0.53237
-0.75	-0.2225578	-0.2169073	-0.144992	-0.2245247	-0.22079
-0.95	0.2692103	0.2811313	0.2895713	0.2645135	0.26845
-0.9945	0.6281614	0.6515622	0.6880045	0.6122589	0.83183
-1.0	0.7189036	0.7720828	0.7875800	0.6038785	-----
-1.10	1.5232443	-0.9275138	1.6559600	1.7551898	-----

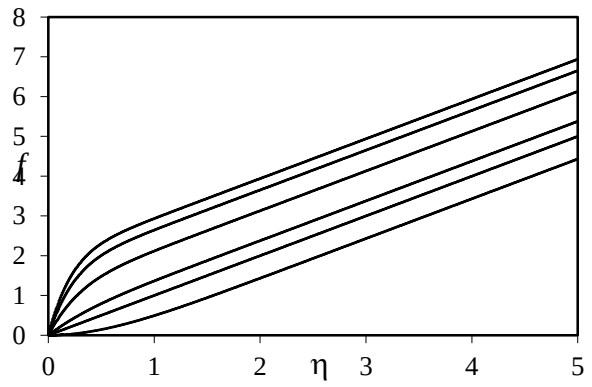

Figure 1: Graph of *f* for the values of α =0,1,2,5, 8 and 10 from bottom

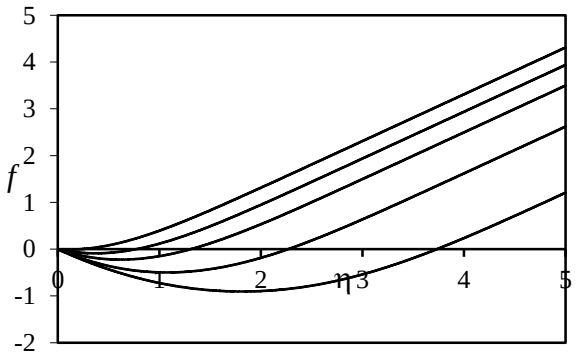

Figure 2: Graph of *f* for the values of α =-0.15, -0.5, -0.75, -0.95 and -1.0 from top

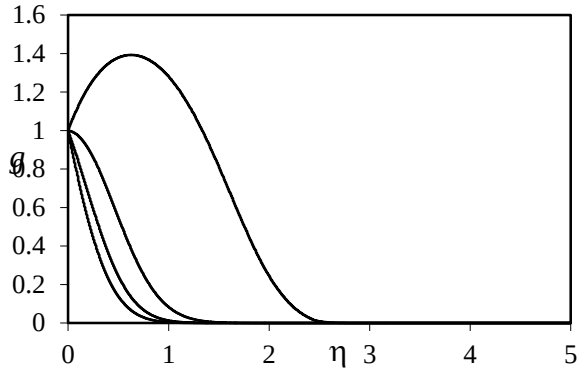

Figure3: Graph of g for α =1, -0.75, -0.95 and -1.0 from top

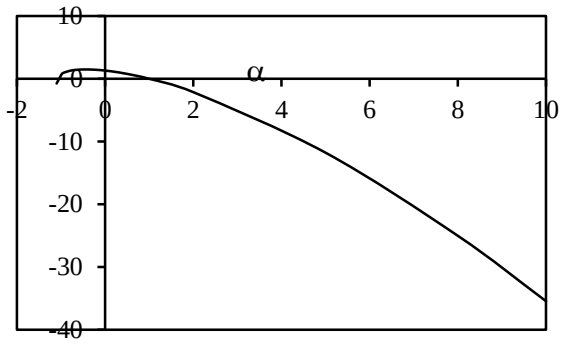

Figure 4: Graph of the skin friction coefficient $f''(0)$

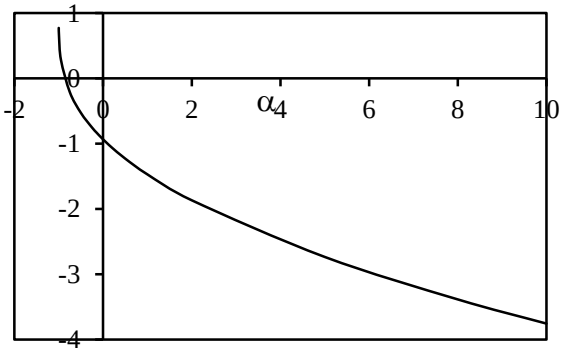

Figure 5: Graph of the gradient of non alignment function *g* i.e. $g'(0)$

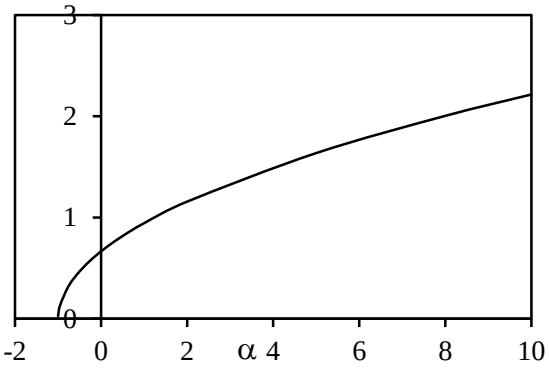

Figure 6: Graph of $-\theta'(0)$ for different values of α when Pr=0.7

REFERENCES

[1] T.C.Chiam, Stagnation Point flow towards a stretching plate, J. Phys. Soc. Japan 63. 1994. 2443-2444.

[2] A. Ishak, R. Nazar and I. Pop, Mixed convection boundary layers in he stagnation point flow toward a stretching vertical sheet , Meccanica ,41. 2006. 509-518.

[3] S. Able, P. H. Veena, K. Rajagopal, V. K. Pravin, non- Newtonian MHD flow over a stretching surface with heat and mass transfer, Int. J. Nonlinear Mech. 39.2004.1067-1078.

[4] A. Ishak, K. Jafar, R. Nazar and I. Pop, MHD stagnation point flow towards a stretching sheet, Physica A 388. 2009. 3377-3383.

[5] Wang. C.Y, Stagnation flow towards a shrinking sheet, International journal of Non-Linear Mechanics, 43,2008. 377 – 382.

[6] T. Hayat, Z. Abbas, M. Sajid, On the Analytic Solution of MHD Flow of a Second Grade Fluid Over a Shrinking Sheet, .J. Appl. Mech. 74(6), 2007, 1165-1171

[7] Tiegang Fang, Boundary layer flow over a shrinking sheet with power-law velocity, International J of Heat and Mass Transfer, 51, 2008, 5838–5843.

[8] S. Nadeem, R Ul Haq, C. Lee, MHD flow of a Casson fluid over an exponentially shrinking sheet, Scientia Iranica B 19,2012, 1550–1553.

[9] Asmat Ara, Najeeb Alam Khan, Hassam Khan, Faqiha Sultan, Radiation effect on boundary layer flow of an Eyring–Powell fluid over an exponentially shrinking sheet, Ain Shams Engineering Journal, V5, 2014, 1337–1342.

[10] K. Zaimi, A. Ishak' I. Pop, Boundary layer flow and heat transfer over a nonlinearly permeable stretching/shrinking sheet in a nanofluid, Scientific Reports 4, Article number: 4404. 2014,

[11] K. Zaimi,, A. Ishak, I. Pop , Flow Past a Permeable Stretching/Shrinking Sheet in a Nano fluid, PLoS ONE 9(11): e111743. 2014,

[12] M. Sajid, T. Hayat, The application of homotopy analysis method for MHD viscous flow due to a shrinking sheet, Chaors Soliton Fractals, 39, 2009, 1317-1323.

[13] Noor, N. F. M., Kechil, S. A. and Hashim, I., Simple non-perturbative solution for MHD viscous flow due to a shrinking sheet, Commun Nonlinear Sci Numer Sim Ilat 15, 2010,144-148.

[14] M. Shafique, F Abbas, A Rashid. Viscous Flow of Micropolar Fluids due to a Shrinking Sheet. I J of Emerging Tech & Adv Engin, 3. 2013. 651-658,.

[15] C. F. Gerald, "Applied Numerical Analysis," Addison- Wesley Publication, New York, 1989.